Dynamics of Ligand Rebinding to Unfolded MbCO by Guanidine HCl

Jaeheung Park, Jooyoung Kim, Taegon Lee, and Manho Lim
Department of Chemistry and Chemistry Institute for Functional Materials, Pusan National University, Busan, Korea

ABSTRACT Femtosecond vibrational spectroscopy was used to probe a functionally important dynamics and residual structure of myoglobin unfolded by 4 M guanidine HCl. The spectra of the dissociated CO indicated that the residual structure of unfolded myoglobin (Mb) forms a few hydrophobic cavities that could accommodate the dissociated ligand. Geminate rebinding (GR) of CO to the unfolded Mb is three-orders-of-magnitude faster and more efficient than the native Mb but similar to a model heme in a viscous solvent, suggesting that the GR of CO to heme is accelerated by the longer retention of the dissociated ligand near the Fe atom by the poorly-structured protein matrix of the unfolded Mb or viscous solvent. The inefficient GR of CO in native Mb, while dissociated CO is trapped in the primary heme pocket located near the active binding site, indicates that the tertiary structure of the pocket in native Mb plays a functionally significant role.

Received for publication 30 January 2008 and in final form 7 March 2008.

Address reprint requests and inquiries to Manho Lim, Tel.: 82-51-510-2243; E-mail: mhlim@pusan.ac.kr.

Unfolded states of proteins are involved in various critical biological phenomena, which range from regulation of the cellular activity to the onset of neurodegenerative diseases (1). The dynamic and structural characterization of unfolded proteins is important for understanding these processes as well as protein folding (1). While the dynamics and structure of folded proteins have been well characterized, those of unfolded proteins are much less understood (2). A detailed investigation of unfolded proteins is often limited by its tendency to aggregate and/or the lack of a dynamic and structural probe (3).

The rebinding of CO to myoglobin (Mb) after photolysis has long been used as a model system for examining the protein dynamics and structure (4). Mb can be readily unfolded without aggregation by adding denaturants. The transient grating and CD signal showed that 4 M Guanidine HCl (GdnHCl) induces complete denaturation of MbCO while heme remains coordinated to the unfolded Mb (5–7). Since the vibrational spectrum of a small ligand is quite sensitive to its surroundings, infrared (IR) spectroscopy of the bound and dissociated ligand can be an excellent probe for examining the details of ligand rebinding dynamics and structures where the dissociated ligand resides (8). Here we probed the rebinding dynamics of CO in GdnHCl-unfolded Mb using fs IR spectroscopy and compared the dynamics with those in native Mb and a model heme, from which a functionally important structural motif in Mb was deduced. The spectra of the dissociated CO were used to probe the residual structure of the unfolded protein.

Fig. 1 shows the transient absorption spectra of the stretching mode of CO bound to and photolyzed from MbCO unfolded by 4 M GdnHCl at 283 K after excitation with a 575 nm pulse (experimental methods are provided in Supplementary Material, Data S1). The negative-going features (bleach, denoted to *A* state), arising from the loss of bound CO, appear faster than the time resolution of the instrument. The bleach spectra, identical to the scaled equilibrium spectrum of the unfolded MbCO, do not evolve with time and its amplitude is proportional to the population of deligated Mb. The lack of time evolution in the bleach spectra suggests that various surroundings of the ligand, which give rise to the broad distribution in the vibrational frequency of bound CO, do not alter the rebinding dynamics of the unfolded Mb. The majority of the bleach recovers in 1 ns, which shows much faster and efficient geminate rebinding (GR) of CO in unfolded Mb than in the native Mb, where only 4% of dissociated CO geminately rebinds within 180 ns (9). The CO rebinding kinetics in the unfolded Mb could be fitted to a kinetic equation describing a three-state model (see Fig. 2 *a*) (9,10): $(0.59 \pm 0.03) \exp\left(-(t/(200 \pm 40)\ \text{ps})^{0.75\pm0.03}\right) + (0.41 \pm 0.03)$. Fig. 2 *a* also shows the GR dynamics of CO to microperoxidase-8 (Mp, a model heme without an organized primary heme pocket) (10,11) in water (1 cP) and an 80:20 (v/v) glycerol/water mixture (73 cP). While CO GR to Mp in water is negligible, the yield and timescale of GR to Mp in viscous solvent were similar to those in the unfolded Mb. The diffusion of dissociated CO is likely to be retarded in the protein matrix of the unfolded Mb (see below) as well as in the viscous solvent. Therefore, the faster and more efficient CO GR can be attributed to the longer retention of dissociated CO near the heme Fe atom by random structures.

Femtosecond IR experiments and time-resolved crystal structures of the photolyzed MbCO at ambient temperature showed that CO becomes temporarily trapped in a nearby heme pocket (denoted to *B* state) before escaping into the surrounding solvent (12–14). The primary heme pocket *B*, in which its surrounding amino-acid residues are highly conserved in mammalian Mb, is located on top of the heme group ~3 Å from the Fe (14–16). The GR of dissociated CO to native Mb is quite inefficient, considering the presence of

Editor: Kathleen B. Hall.

doi: 10.1529/biophysj.108.130641

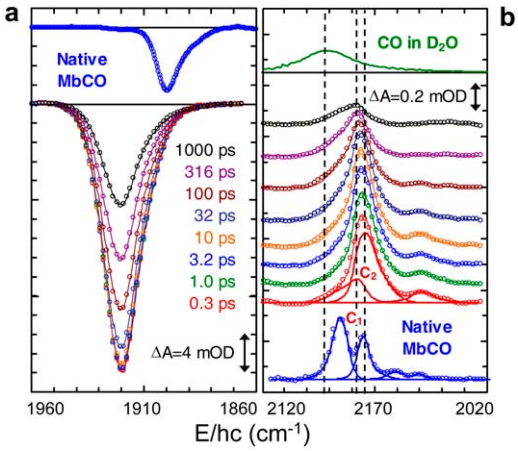

FIGURE 1 Representative time-resolved vibrational spectra of the CO bound (*a*) to and photolyzed (*b*) from MbCO unfolded by 4 M Guanidine HCl. The corresponding spectra of the native MbCO and CO dissolved in D_2O are also shown for comparison. The data of the bound CO (○) were fit to the sum of three Gaussians. The data of photolyzed CO (○) were fit to two bands (C_1 and C_2) plus their hot bands (see text). The dotted vertical lines are shown to indicate the peak positions of the solvated CO, C_1, and C_2 band. For clarity, the quadratic background was subtracted from the measured spectra. The spectra of photolyzed CO were offset to avoid overlap.

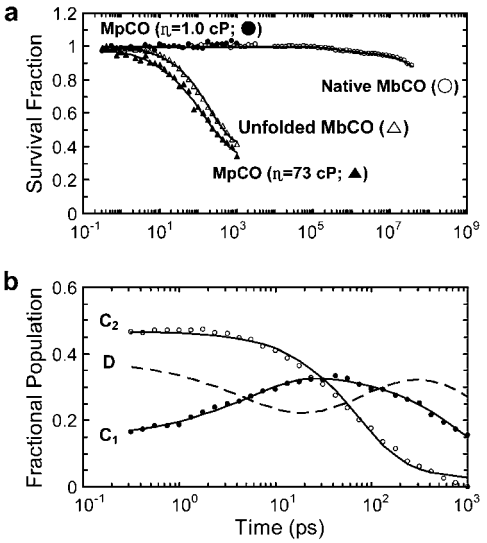

FIGURE 2 (*a*) Change in the survival population of the deligated heme in native MbCO, MpCO, and the unfolded MbCO after photolysis. The rebinding kinetics is well described by the three-state kinetic model (*solid lines*). (*b*) The change in fractional population of each state for dissociated CO in the unfolded Mb (the *solid lines* are the fit to the scheme in text).

the ligand in close proximity to the Fe for hundreds of nanoseconds (12,14,17). The primary heme pocket, a specific local tertiary structure of Mb formed by the highly conserved residues, is likely to be destroyed in the unfolded Mb. The much faster and efficient CO GR in the unfolded Mb can be attributed to the destruction of the primary heme pocket. It is consistent with the suggestion that the primary heme pocket plays a significant role in suppressing CO rebinding by constraining the ligand spatially and orientationally (12).

The positive-going features (Fig. 1 *b*) appear <0.3 ps after photolysis, indicating that they arise from the CO in close proximity to Fe. They are similar to but different in detail from the *B*-state spectra of native MbCO (8,12,18). They are also different from the spectrum of CO dissolved in D_2O (17). Hence, they were assigned to CO residing within protein matrix of the unfolded Mb after photolysis. They were denoted as the *C* states to differentiate them from the *B* states describing the ligand states in the well-structured primary heme pocket of native Mb. The *C* state exhibits strong spectral evolution, which is well described by two bands (denoted C_1 and C_2) plus their red-shifted replicas with changing amplitudes (Figs. 1 *b* and 2 *b*) (19,21). Skewed band shape, comprised of the sum of two (C_1) or three (C_2) Gaussians, likely reflects the CO residing in the assembly of many ill-structured cavities of the unfolded Mb, where a measurable fraction of CO can accumulate at some point in time. Although the C_2 band decays nonexponentially with time, the C_1 band initially grows with a few ps, maintains its magnitude for 10–100 ps, and decays slowly in hundreds-of-picoseconds timescale. The growth of the C_1 band can be attributed to the diffusion of CO to the farther cavities from the Fe. Each *C* state may involve several ill-structured cavities with similar characteristics such as a comparable distance from the Fe. While the CO in the cavities can have apparent spectral bands, the CO in the protein matrix with a small population and CO diffusing between cavities will not form a detectable spectral band due to inhomogeneous broadening. Thus, the dissociated CO not forming an apparent spectrum is denoted as the *D* (dark) state. A kinetic scheme including the interconversion among and rebinding from the three states (C_1, C_2, and *D*) was used to fit the kinetics of the *C* state spectra. A kinetic scheme and parameters recovered from the global fit to the entire spectra of both photolyzed CO and bound CO are as follows (20):

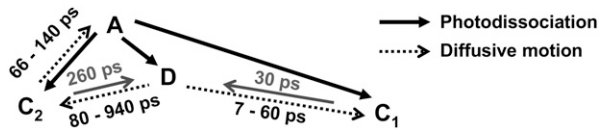

SCHEME 1

The ratio for the extinction coefficient of the bound CO and photolyzed CO was fitted to 34 ± 2, similar to 33 ± 1 in native Mb (18), validating the scheme. The initial partitioning of photolyzed CO, also recovered from the fit, was 15 ± 3% in C_1, 47 ± 5% in C_2, and 38 ± 4% in *D*. According to this scheme, photolysis leads from *A* to mainly C_2 and *D*, C_1 initially builds up due to diffusion from *D* but decays to *D*, and CO rebinds primarily from C_2. It can be envisioned that C_2 (C_1) involves hydrophobic cavities near (far from) the Fe. At a later pump-probe delay a larger fraction of unbound CO is found in *D* (see Fig. 2 *b*), indicating that dissociated CO

diffuses into the unfolded protein matrix where no apparent spectrum can be observed. There was no evidence for a solvated CO up to 1 ns after photolysis, suggesting that dissociated CO either rebinds or remains inside the unfolded protein matrix for at least 1 ns.

While the above kinetic scheme results in a reasonable physical explanation for the dissociated CO, it cannot be a unique solution. A more elaborate kinetic scheme involving more cavities may describe the data as well. However, the poorly-resolved spectral shape does not warrant a more complex scheme. It was found inappropriate to consider the band near 2070 cm^{-1} as a whole and contribute the spectral evolution to the conformational relaxation of the unfolded Mb after de-ligation instead of the motion of CO among cavities (detailed discussion is given in Data S1).

The extent of the denaturation of Mb monitored by CD and the transient grating (sensitive to the secondary and tertiary structures, respectively) showed that the signal change is complete at 4 M GdnHCl (5,7). One might think the heme group of the unfolded Mb by 4 M GdnHCl is well exposed to the solvent. However, the lack of solvated CO spectra after photolysis suggests that the distal side of heme might still be well buried within the randomly coiled polypeptide of Mb. It is consistent with the ultrafast appearance of the spectra for the dissociated CO within the protein matrix. Clearly, the ill-structured protein matrix of the unfolded Mb surrounds the distal side of the heme, which delays the diffusion of dissociated CO, and accelerates its GR, implying that the tertiary structure of the primary heme pocket in native Mb is arranged in a way to suppress CO GR while holding it near the Fe for hundreds of nanoseconds.

SUPPLEMENTARY MATERIAL

To view all of the supplemental files associated with this article, visit www.biophysj.org.

ACKNOWLEDGMENTS

This work was supported by the Korea Science and Engineering Foundation (KOSEF) grant funded by the Korean government (MOST) (No. R01-2007-000-20853-0).

REFERENCES and FOOTNOTES

1. Klein-Seetharaman, J., M. Oikawaz, S. B. Grimshaw, J. Wirmer, E. Duchardt, T. Ueda, T. Imoto, L. J. Smith, C. M. Dobson, and H. Schwalbe. 2002. Long-range interactions within a nonnative protein. *Science*. 295:1719–1722.
2. Dobson, C. M., A. Sali, and M. Karplus. 1998. Protein folding: a perspective from theory and experiment. *Angew. Chem. Int. Ed.* 37:869–893.
3. Shortle, D., and M. S. Ackerman. 2001. Persistence of native-like topology in a denatured protein in 8 M urea. *Science*. 293:487–489.
4. Springer, B. A., S. G. Sligar, J. S. Olson, and G. N. Phillips, Jr. 1994. Mechanisms of ligand recognition in myoglobin. *Chem. Rev.* 94:699–714.
5. Hargrove, M. S., and J. S. Olson. 1996. The stability of holomyoglobin is determined by heme affinity. *Biochemistry*. 35:11310–11318.
6. Moczygemba, C., J. Guidry, and P. Wittung-Stafshede. 2000. Heme orientation affects holo-myoglobin folding and unfolding kinetics. *FEBS Lett*. 470:203–206.
7. Choi, J., and M. Terazima. 2002. Denaturation of a protein monitored by diffusion coefficients. *Myoglob. J. Phys. Chem. B*. 106:6587–6593.
8. Kim, S., J. Heo, and M. Lim. 2005. Conformational dynamics of heme pocket in myoglobin and hemoglobin. *Bull. Korean Chem. Soc*. 26:151–156.
9. Henry, E. R., J. H. Sommer, J. Hofrichter, and W. A. Eaton. 1983. Geminate recombination of carbon monoxide to myoglobin. *J. Mol. Biol*. 166:443–451.
10. Cao, W., X. Ye, G. Y. Georgiev, S. Berezhna, T. Sjodin, A. A. Demidov, W. Wang, J. T. Sage, and P. M. Champion. 2004. Proximal and distal influences on ligand binding kinetics in microperoxidase and heme model compounds. *Biochemistry*. 43:7017–7027.
11. Aron, J., D. A. Baldwin, H. M. Marques, J. M. Pratt, and P. A. Adams. 1986. Hemes and hemoproteins. 1. Preparation and analysis of the heme-containing octapeptide (microperoxidase-8) and identification of the monomeric form in aqueous solution. *J. Inorg. Biochem*. 27: 227–243.
12. Lim, M., T. A. Jackson, and P. A. Anfinrud. 1997. Ultrafast rotation and trapping of carbon monoxide dissociated from myoglobin. *Nat. Struct. Biol*. 4:209–214.
13. Srajer, V., Z. Ren, T.-Y. Teng, M. Schmidt, T. Ursby, D. Bourgeois, C. Pradervand, W. Schildkamp, M. Wulff, and K. Moffat. 2001. Protein conformational relaxation and ligand migration in myoglobin: a nanosecond to millisecond molecular movie from time-resolved Laue x-ray diffraction. *Biochemistry*. 40:13802–13815.
14. Schotte, F., J. Soman, J. S. Olson, M. Wulff, and P. A. Anfinrud. 2004. Picosecond time-resolved x-ray crystallography: probing protein function in real time. *J. Struct. Biol*. 147:235–246.
15. Schlichting, I., J. Berendzen, G. N. Phillips, Jr., and R. M. Sweet. 1994. Crystal structure of photolyzed carbonmonoxy-myoglobin. *Nature*. 371:808–812.
16. Teng, T. Y., V. Srajer, and K. Moffat. 1994. Photolysis-induced structural changes in single crystals of carbonmonoxy myoglobin at 40 K. *Nat. Struct. Biol*. 1:701–705.
17. Jackson, T. A. 1996. Probing the dynamics of ligand motion in myoglobin and hemoglobin using time-resolved mid-IR spectroscopy. *In* Chemistry. Harvard University, Cambridge, MA.
18. Lim, M., T. A. Jackson, and P. A. Anfinrud. 1995. Mid-infrared vibrational spectrum of CO after photodissociation from heme: evidence for a ligand docking site in the heme pocket of hemoglobin and myoglobin. *J. Chem. Phys*. 102:4355–4366.
19. The red-shifted replica was attributed to the hot band because it is red-shifted by 26 ± 1 cm^{-1}, similar to the anharmonicity of CO in the gas phase, 25.3 cm^{-1}, and it decays with a time constant of 270 ± 50 ps, comparable to the vibrational relaxation time of CO in the primary heme pocket (21). The nascent vibrationally excited CO population was 5 ± 1%, also similar to the value obtained in native Mb (8,18).
20. The time dependence of the integrated absorbance contains information on the GR rates, transitions among states, and the vibrational relaxation of the excited CO. The time-independent rate constants involving all rebinding from and interconversion among the three states cannot reproduce the *C*-state kinetics. A stretched exponential function was used to account for the diffusive nature of ligand motion and/or the distribution of rates reflecting transitions from many cavities. Since CO moving out from cavities toward *D* will results in immediate spectral loss, the transition rate to *D* from *C* is set time-independent. The transition rates found to be too slow to be of any consequence were set to 0. The inverse rate coefficients are given along the arrow. The values in the diffusive motion correspond to those at 0.3 ps and 1 ns.
21. Sagnella, D. E., J. E. Straub, T. A. Jackson, M. Lim, and P. A. Anfinrud. 1999. Vibrational population relaxation of carbon monoxide in the heme pocket of photolyzed carbonmonoxy myoglobin: comparison of time-resolved mid-IR absorbance experiments and molecular dynamics simulations. *Proc. Natl. Acad. Sci. USA*. 96:14324–14329.